Journal Article

Diffraction in volume reflection gratings with variable fringe contrast

Brotherton-Ratcliffe, D., Bjelkhagen, H., Osanlou, A. and Excell, P.

Diffraction in volume reflection gratings with variable fringe contrast

David Brotherton-Ratcliffe,[1,2,3*] Hans Bjelkhagen,[1] Ardeshir Osanlou,[1] Peter Excell[1]

[1]*Centre for Applied Photonics, Applied Science, Computing and Engineering, Glyndŵr University, Mold Road, Wrexham, Wales, LL1 2AW, UK*
[2]*Geola Technologies Ltd, Sussex Innovation Centre, Science Park Square, Falmer, East Sussex, BN1 9SB, UK*
[3]*Geola Digital UAB, Naugarduko g.41, Vilnius 03227, Lithuania*
**Corresponding author: dbr@geola.co.uk*

Received Month X, XXXX; revised Month X, XXXX; accepted Month X, XXXX; posted Month X, XXXX (Doc. ID XXXXX); published Month X, XXXX

The PSM model is used to analyze the process of diffraction occurring in volume reflection gratings in which fringe contrast is an arbitrary function of distance within the grating. General analytic expressions for diffraction efficiency at Bragg resonance are obtained for unslanted panchromatic lossless reflection gratings at oblique incidence. These formulae are then checked, for several diverse fringe contrast profiles with numerical solutions of the Helmholtz equation where exceptionally good agreement is observed. Away from Bragg resonance the case of the hyperbolically decaying fringe contrast profile is shown to lead to an analytic expression for the diffraction efficiency and this is again compared successfully with numerical solutions of the Helmholtz equation.
OCIS codes: (090.0090) Holography; (050.1960) Diffraction Theory
http://dx.doi/org/10.1364/AO.99.099999

1.Introduction

Volume reflection gratings are often produced by laser irradiation of a silver halide holographic emulsion and subsequent chemical processing. During the chemical processing stage, diffusion of the processing chemicals occurs from only one side of the grating. This leads to a fringe contrast that decays with emulsion penetration depth (1).

In addition, photopolymer materials are subject to a similar effect due to the unexposed photopolymer material possessing an often rather high absorption coefficient that is caused by the sensitizing dyes employed. Optical absorption during recording of the grating can therefore affect index modulation, resulting once again in a variable fringe contrast profile.

Current analytic models of diffraction in volume gratings only describe gratings having a constant fringe contrast (2,3). Here we shall use the parallel stacked mirror model (PSM) (3-9) to develop analytic expressions for the diffraction efficiency at Bragg resonance describing gratings with a very general fringe contrast profile. In particular we shall show that at Bragg resonance, a reflection grating possessing a general analytic fringe contrast profile exhibits the same diffractive properties as an equivalent grating of constant fringe contrast but of differing thickness. Away from Bragg resonance this equivalence rule breaks down but we are still able to find an analytic solution for the case of a hyperbolically decaying fringe contrast profile, which broadly corresponds to the expected form for silver halide.

2.PSM model of the normal-incidence unslanted monochromatic reflection grating

For simplicity and for clarity of exposition we start with the simple case of the normal-incidence unslanted reflection grating under monochromatic illumination. A general harmonic index grating with arbitrary fringe contrast, in this case, may be expressed as

$$n = n_0 + \frac{n_1}{2}\left\{e^{2i\alpha\beta y} + e^{-2i\alpha\beta y}\right\}\gamma(y) \qquad (1)$$

Here $\gamma(y)$ is an arbitrary function describing the fringe contrast, n_0 is the average (external and internal) index, n_1 is the index modulation and y is the normal distance into the grating. The parameters, α and β are respectively the ratio of the replay wavelength (λ_c) to recording wavelength (λ_r) and the propagation constant and are given by

$$\alpha = \lambda_c / \lambda_r \;\; ; \;\; \beta = \frac{2\pi n_0}{\lambda_c} \qquad (2)$$

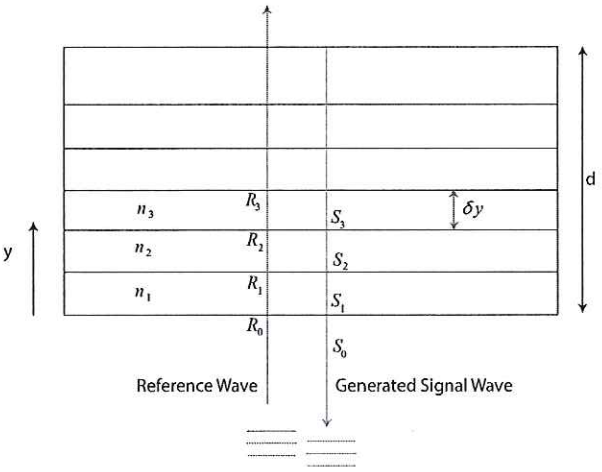

Fig.1 Unslanted reflection grating shown illuminated by a reference wave, R which provokes a signal wave, S. The grating has thickness,d and the refractive index within the grating is a general harmonic function. The index outside the grating is n_0.

We now wish to understand the response of the grating to a plane reference wave of the form

$$R^{ext} = e^{i\beta y} \tag{3}$$

We assume that the grating is surrounded by a zone of constant index, n_0 and start by modeling the grating of Equation (1) by a series of many thin constant-index layers, n_0, n_1, n_2, ..., n_M, between each of which exists an index discontinuity (see Fig. 1). Across each such discontinuity we may derive the well-known Fresnel formulae for the amplitude reflection and transmission coefficients from Maxwell's equations by demanding that the tangential components of the electric and magnetic fields be continuous.

An illuminating plane wave will in general generate many mutually interfering reflections from each discontinuity. We therefore imagine two plane waves within the grating – the driving reference wave, R(y) and a created signal wave, S(y). Using the Fresnel formulae we may then write, for either the σ- or the π-polarisation, the following recurrence relations:

$$\begin{aligned} R_J &= 2e^{i\beta n_J \delta y/n_0}\left\{\frac{n_{J-1}}{n_J + n_{J-1}}\right\}R_{J-1} + e^{i\beta n_J \delta y/n_0}\left\{\frac{n_{J-1} - n_J}{n_J + n_{J-1}}\right\}S_J \\ S_J &= 2e^{i\beta n_J \delta y/n_0}\left\{\frac{n_{J+1}}{n_{J+1} + n_J}\right\}S_{J+1} + e^{i\beta n_J \delta y/n_0}\left\{\frac{n_{J+1} - n_J}{n_{J+1} + n_J}\right\}R_J \end{aligned} \tag{4}$$

Here the terms in curly brackets are just the Fresnel amplitude reflection and transmission coefficients and the exponential is a phase propagator that advances the phase of the R and S waves as they travel the distance δy between discontinuities. We now let

$$X_{J-1} = X_J - \frac{dX}{dY}\delta y - \ldots \tag{5}$$

where X represents R, S or n and we consider the limit $\delta y \to 0$. Further expanding the exponential terms as Taylor series and ignoring quadratic and higher order terms in δy we arrive at the differential counter-part to Equation (4)

$$\begin{aligned} \frac{dR}{dy} &= \frac{R}{2}\left\{2i\beta - \frac{1}{n}\frac{dn}{dy}\right\} - \frac{1}{2n}\frac{dn}{dy}S \\ \frac{dS}{dy} &= -\frac{S}{2}\left\{2i\beta + \frac{1}{n}\frac{dn}{dy}\right\} - \frac{1}{2n}\frac{dn}{dy}R \end{aligned} \tag{6}$$

These are the basic equations on which the PSM model for the unslanted normal-incidence reflection grating is based. For the case of monochromatic illumination of the grating, the PSM model splits the total electric field into a signal wave of amplitude S(y) and into a reference wave of amplitude R(y) (see Fig.1). Equations (6) then provide us with a description of how these two waves behave and interact within the grating. These equations are in fact an exact representation of Maxwell's equations. We will now solve them for the index function of equation (1) by making some reasonable approximations.

We start by making the transformation

$$R \to R'(y)e^{i\beta y} \quad ; \quad S \to S'(y)e^{-i\beta y} \tag{7}$$

and using

$$\begin{aligned} \overline{R} &= \langle R' \rangle \\ \overline{S} &= \langle S' \rangle \end{aligned} \tag{8}$$

Here, triangular brackets operate on a harmonic or quasi-harmonic quantity and indicate an average over several cycles of the respective function, X such that

$$< X > \equiv \frac{1}{\ell}\int_y^{y+\ell} X(y')dy' \tag{9}$$

where ℓ is greater than several periods (typically >3) but much smaller than the emulsion thickness, d. Equations (6) then reduce to

$$\begin{aligned} \frac{d\overline{R}(y)}{dy} &= -\frac{1}{2n_0}\frac{n_1}{2}\left\{\begin{bmatrix} 2i\alpha\beta\gamma(y) \\ +\gamma'(y) \end{bmatrix} e^{2i(\alpha-1)\beta y}\right\}\overline{S}(y) \\ \frac{d\overline{S}(y)}{dy} &= -\frac{1}{2n_0}\frac{n_1}{2}\left\{\begin{bmatrix} -2i\alpha\beta\gamma(y) \\ +\gamma'(y) \end{bmatrix} e^{-2i(\alpha-1)\beta y}\right\}\overline{R}(y) \end{aligned} \tag{10}$$

Now if the contrast function is slowly varying compared to the harmonic index modulation, it is clear that

$$|\gamma'(y)| << |2i\alpha\beta\gamma(y)| \tag{11}$$

and equations (10) reduce further to

$$\frac{d\bar{R}(y)}{dy} = -i\alpha\kappa\gamma(y)\bar{S}(y)e^{2i\beta y(\alpha-1)}$$
$$\frac{d\bar{S}(y)}{dy} = i\alpha\kappa\gamma(y)\bar{R}(y)e^{-2i\beta y(\alpha-1)} \quad (12)$$

where we have introduced Kogelnik's constant

$$\kappa = \frac{n_1\pi}{\lambda_c} \quad (13)$$

Following (3) we introduce the pseudo-field

$$\hat{S} = \bar{S}e^{2i\beta y(\alpha-1)} \quad (14)$$

whereupon equations (12) reduce to

$$c_R\frac{d\bar{R}(y)}{dy} = -i\kappa\gamma(y)\hat{S}(y)$$
$$c_S\frac{d\hat{S}(y)}{dy} = -i\vartheta\hat{S}(y) - i\kappa\gamma(y)\bar{R}(y) \quad (15)$$

with

$$\vartheta = 2\frac{\beta}{\alpha}(\alpha-1) \;\; ; \;\; c_R = -c_S = \frac{1}{\alpha} \quad (16)$$

At Bragg Resonance where $\alpha = 1$ equation (15) has the following analytic solution for the diffraction efficiency, η, which is valid for the reflection boundary conditions R(0)=1, S(d)=0

$$\eta = \left|\frac{c_S}{c_R}\right| S(0)S^*(0) = \tanh^2\left[\kappa\int_0^d \gamma(y)\,dy\right] \quad (17)$$

This should be compared to the well-known formula for a constant fringe contrast of

$$\eta = \tanh^2[\kappa d] \quad (18)$$

We can therefore rewrite equation (17) as

$$\eta = \tanh^2\left[\kappa d_{eff}\right] \quad (19)$$

where d_{eff} is an effective grating thickness given by

$$d_{eff} = \int_0^d \gamma(y)\,dy \quad (20)$$

In order to check equation (17) we first use a standard Gaussian form for the contrast function, giving the following index

$$n = n_0 + n_1 e^{-\frac{\omega y^2}{d^2}}\cos(2\beta y) \quad (21)$$

Equation (17) then reduces to

$$\eta = \tanh^2\left[\frac{1}{2}d\kappa\sqrt{\frac{\pi}{\omega}}erf\left[\sqrt{\omega}\right]\right] \quad (22)$$

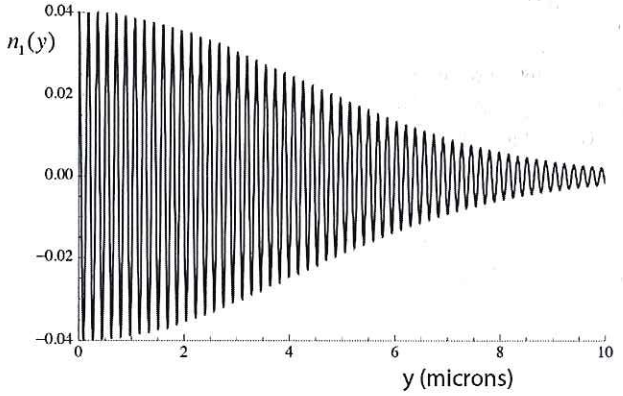

Fig.2 Harmonic grating profile with Gaussian decaying fringe contrast function (equation (21)). Recording wavelength 532nm. n_1=0.04, d=10 microns.

Fig.2 shows an example of the grating of equation (21) for an omega value of 3. This represents a typical silver halide grating of typical grating modulation and typical grating thickness. The choice of an omega value of 3 corresponds to a pronounced chemical diffusion effect where the efficiency of chemical processing starts to decay visibly after a penetration of only two microns. Fig.3 shows the corresponding diffraction efficiency versus grating thickness as calculated by equation (22) where it is compared to a numerical Runge-Kutta integration of the Helmholtz equation. Clearly the analytic result is extremely accurate.

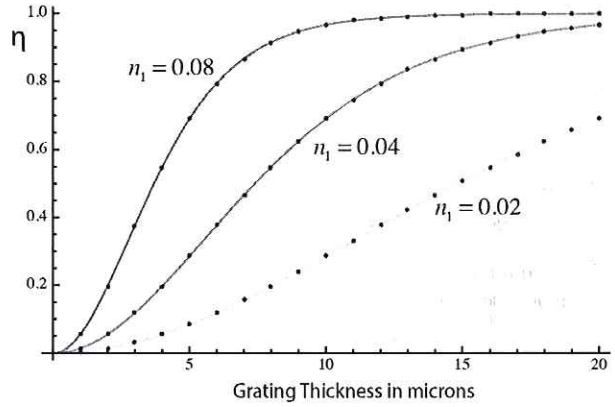

Fig.3 Graph showing diffraction efficiency versus grating thickness of an unslanted normal incidence reflection grating with the Gaussian tapering harmonic index modulation of Equation (21) (see Fig.2). The continuous lines represents the PSM analytic formula (Equation (22)) with ω=3 and the points represent a full Runge-Kutta integration of the Helmholtz equation. Three values of the index modulation are plotted: $n_1(0)$=0.02, $n_1(0)$=0.04 and $n_1(0)$=0.08. Gratings recorded and played back at 532nm. n_0=1.5.

To test equation (17) further we use the more extreme contrast function

$$n = n_0 + \frac{n_1}{2}\left(1+\cos\left(\frac{\sigma\pi y}{2d}\right)e^{-\frac{\omega y^2}{d^2}}\right)\cos(2\beta y) \quad (23)$$

In this case equation (17) reduces to

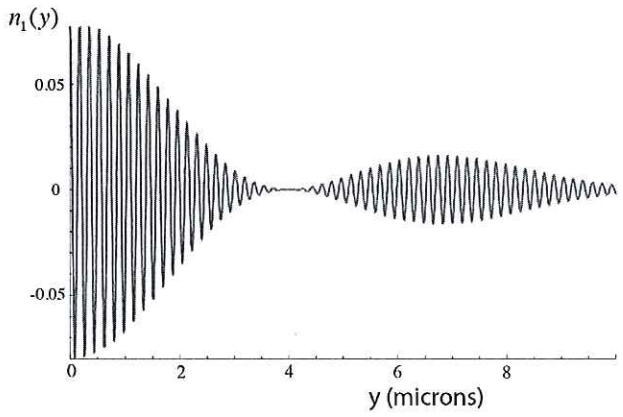

Fig.4 Harmonic grating profile with Gaussian oscillatory fringe contrast function (equation(23)). Recording wavelength 532nm. n_1=0.08, d=10 microns.

$$\eta = \tanh^2\left(\frac{\kappa d\sqrt{\pi}}{8\sqrt{\omega}}\left(\begin{array}{l} 2erf\left[\sqrt{\omega}\right]+ \\ e^{-\frac{\pi^2\sigma^2}{16\omega}}\left(\begin{array}{l} erf\left[\dfrac{4\omega-i\pi\sigma}{4\sqrt{\omega}}\right]+ \\ erf\left[\dfrac{4\omega+i\pi\sigma}{4\sqrt{\omega}}\right] \end{array}\right) \end{array}\right)\right) \quad (24)$$

Fig.4 shows an example of this grating for an omega value of 3 and for a sigma value of 5. The physical significance of this profile is less immediately obvious than that of Fig.2 although it does show a worsened chemical diffusion effect. The physical significance of the second smaller peak in fringe contrast can be thought of - very approximately - as representing the interaction of the main chemical diffusion process occurring from the front surface of the grating, with a (non-constant) optical absorption effect caused by a finite absorption present in the photographic material at recording, acting on both reference and object beams. However, although this constitutes a plausible explanation, the primary reason for the choice of this more extreme example is to demonstrate the validity of the key assumption of equation (11) for an extreme example.

Fig.5 shows the corresponding diffraction efficiency versus grating thickness as calculated by equation (24) where it is once again compared to a numerical Runge-Kutta integration of the Helmholtz equation. Clearly the analytic result is again extremely accurate, even for this harmonic contrast function that must be interpreted as an extreme case.

Away from Bragg resonance equation (17) is not valid. Here we cannot find a general analytic formula for the diffraction efficiency valid for an arbitrary fringe contrast profile. However we are able to solve equation (15) for various specific contrast profiles which are nevertheless suitable for describing typically expected fringe contrast distributions for the silver halide chemical processing effect. For example the contrast function

$$\gamma(y) = \frac{1}{1+ay} \quad (25)$$

leads to a diffraction efficiency of

$$\eta = \left|\frac{c_S}{c_R}\right| S(0)S^*(0) \quad (26)$$

where

$$S(0) = \left(\frac{i\alpha\vartheta}{a}\right)^{-\frac{1}{2}-\frac{\alpha\kappa}{a}} \times$$

$$\frac{\left\{\begin{array}{l} (-1-ad)\Omega_0\alpha\vartheta\left(\dfrac{i\alpha\vartheta}{a}\right)^{\frac{1}{2}+\frac{\alpha\kappa}{a}}\Omega_3\left(\vartheta\Omega_5+i\kappa\Omega_6\right)+ \\ \alpha\vartheta\Omega_9\left(\begin{array}{l} \sqrt{\pi}\left(\dfrac{i\alpha\vartheta}{a}\right)^{\frac{\alpha\kappa}{a}}\Omega 1\left(\vartheta\Omega_5+i\kappa\Omega_6\right)+ \\ \left(-\sqrt{\pi}\left(\dfrac{i\alpha\vartheta}{a}\right)^{\frac{\alpha\kappa}{a}}\Omega_2+e^{\frac{i\alpha\vartheta}{2a}}\sqrt{\dfrac{i\alpha\vartheta}{a}}\Omega_4\right)\times \\ \left(i\kappa\Omega_7+(1+ad)\vartheta\Omega_8\right) \end{array}\right) \end{array}\right\}}{\sqrt{\dfrac{i\alpha\vartheta}{a}}} \quad (27)$$

$$\left\{\begin{array}{l} (-1-ad)\Omega_0\alpha\vartheta\kappa\Omega_3\Omega_6 \\ +a\sqrt{\pi}\Omega_9\left(\begin{array}{l} -i\kappa\Omega_1\Omega_6+ \\ \Omega_2\left(i\kappa\Omega_7+(1+ad)\vartheta\Omega_8\right) \end{array}\right) \end{array}\right\}$$

and where the Omega functions are given in Appendix A. Fig.6 shows an example of the fringe contrast function of equation (25). In Fig.7 we plot the corresponding diffraction efficiency of this grating versus replay wavelength along with a Runge-Kutta integration of the Helmholtz equation, where excellent agreement is observed.

Another useful fringe contrast function which is associated with an analytic expression for the diffraction efficiency is the simple exponential decay

$$\gamma(y) = e^{-\sigma y} \quad (28)$$

Here a rather complex solution is available in terms of Bessel functions of the first kind.

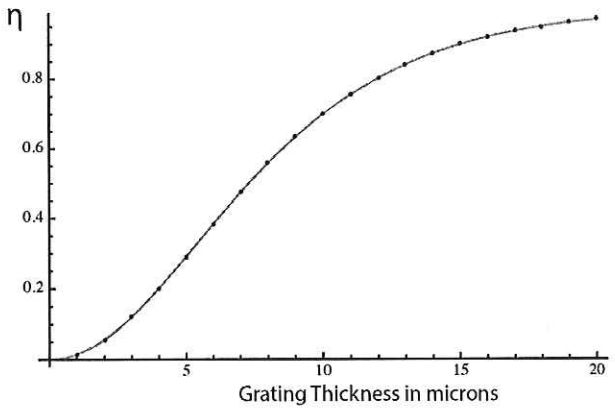

Fig.5 Graph showing diffraction efficiency versus grating thickness of an unslanted normal incidence reflection grating with the Gaussian oscillating harmonic index modulation of Equation (23) (see Fig.4). The continuous line represents the PSM analytic formula (Equation(24)) and the points represent a full Runge-Kutta integration of the Helmholtz equation. Grating recorded and played back at 532nm. n_0=1.5.

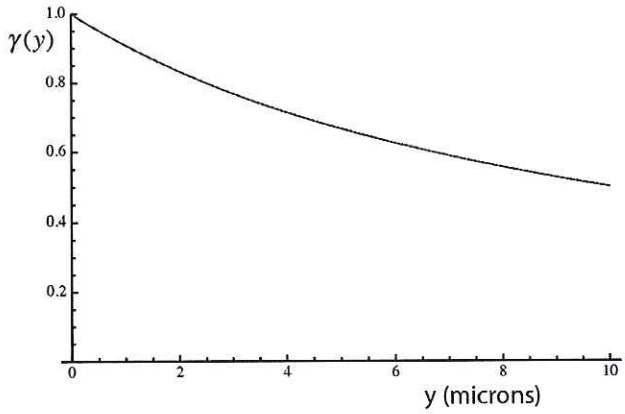

Fig.6. Example of the fringe contrast profile of equation (25) with a value of the parameter, a =100,000.

3.Unslanted multi-chromatic gratings at normal incidence

The above discussion can be extended in a fairly trivial fashion to the case of multi-chromatic recording and reconstruction. Equation (1) generalizes to

$$n = n_0 + \sum_{k=1}^{N} \frac{n_k}{2}\left\{e^{2i\alpha_k\beta y} + e^{-2i\alpha_k\beta y}\right\}\gamma_k(y) \qquad (29)$$

Following (3) and assuming that the individual gratings labeled by the subscript k have very different spatial frequencies Equation (12) then reduces to

$$\begin{aligned}
&\frac{d\bar{R}(y)}{dy} = -i\left\langle \bar{S}(y)\sum_{k=1}^{N}\alpha_k\kappa_k\gamma_k(y)e^{2i\beta y(\alpha_k-1)}\right\rangle \\
&= -i\bar{S}(y)\alpha_m\kappa_m\gamma_m(y)e^{2i\beta y(\alpha_m-1)} \\
&\frac{d\bar{S}(y)}{dy} = i\bar{R}(y)\left\langle\sum_{k=1}^{N}\alpha_k\kappa_k\gamma_k(y)e^{-2i\beta y(\alpha_k-1)}\right\rangle \\
&= i\bar{R}(y)\alpha_m\kappa_m\gamma_m(y)e^{-2i\beta y(\alpha_m-1)}
\end{aligned} \qquad (30)$$

Here the subscript m indicates that the alpha, kappa and gamma parameters belong to the grating closest to Bragg resonance with the illuminating S wave. Basically all other gratings are simply averaged out by the triangular brackets!

Applying the same procedure as above we then deduce an expression for the diffraction efficiency when a multi-chromatic grating is illuminated with one of its component recording wavelengths

$$\eta = \left|\frac{c_S}{c_R}\right| S(0)S^*(0) = \tanh^2\left[\kappa_m\int_0^d \gamma_m(y)\,dy\right] \qquad (31)$$

4.Unslanted gratings at oblique incidence

When the reference wave is incident to the grating at an oblique angle, equation (6) must be replaced by the following more general PSM equations (3,6) which are valid for a σ-polarization

$$\begin{aligned}
&\sin\theta_c\frac{\partial R}{\partial x} + \cos\theta_c\frac{\partial R}{\partial y} = \\
&\frac{R}{2}\left\{2i\beta - \frac{1}{n\cos\theta_c}\frac{\partial n}{\partial y}\right\} - \frac{S}{2}\left\{\frac{1}{n\cos\theta_c}\frac{\partial n}{\partial y}\right\} \\
&\sin\theta_c\frac{\partial S}{\partial x} - \cos\theta_c\frac{\partial S}{\partial y} = \\
&\frac{S}{2}\left\{2i\beta + \frac{1}{n\cos\theta_c}\frac{\partial n}{\partial y}\right\} + \frac{R}{2}\left\{\frac{1}{n\cos\theta_c}\frac{\partial n}{\partial y}\right\}
\end{aligned} \qquad (32)$$

It should be pointed out here that an approximation of constant ray direction has been made in arriving at these equations and as such they constitute an approximate solution of Maxwell's equations (3).

We may now apply a similar method to that applied to the normal incidence case in section 2. Firstly we adopt a modified grating equation

$$n = n_0 + \frac{n_1}{2}\left\{e^{2i\alpha\beta\cos\theta_r y} + e^{-2i\alpha\beta\cos\theta_r y}\right\}\gamma(y) \qquad (33)$$

where θ_r is now the angle of incidence on recording. Secondly the transformation of equation (7) must be generalized to

$$R \to R'(y)e^{i\beta(\sin\theta_c x + \cos\theta_c y)} \quad ; \quad S \to S'(y)e^{i\beta(\sin\theta_c x - \cos\theta_c y)} \qquad (34)$$

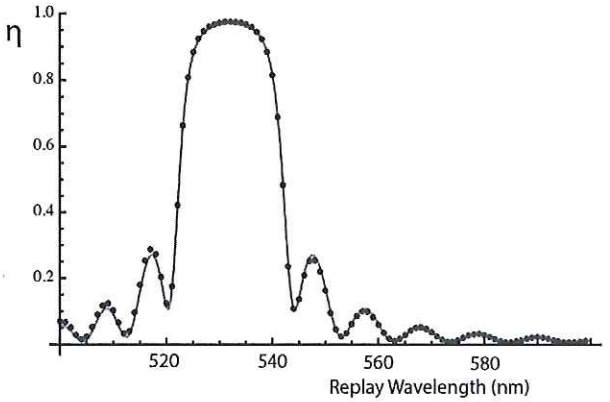

Fig.7. Diffraction efficiency versus replay wavelength for the hyperbolically decaying fringe contrast function of equation (25) and Fig.6. Recording wavelength 532nm. n_0=1.5. n_1=0.06. Red solid line is the analytic result of equation (27) and blue circles represent a Runge-Kutta integration of the Helmholtz equation.

The same mathematical steps then show that equation (32) simplifies directly to equation (15), but where now

$$\vartheta = 2\beta(1-\frac{\cos\theta_c}{\alpha\cos\theta_r})\cos^2\theta_c \;\; ; \;\; c_R = -c_S = \frac{\cos^2\theta_c}{\alpha\cos\theta_r} \qquad (35)$$

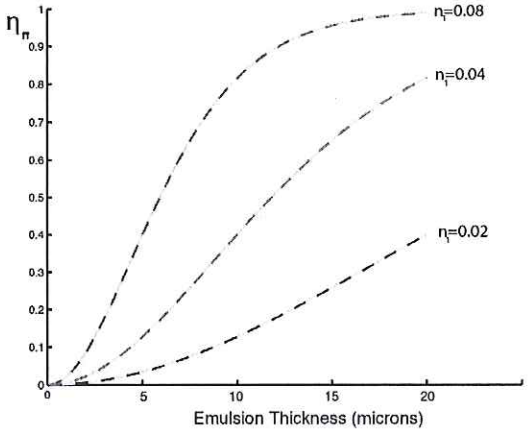

Fig.8 Diffraction efficiency at Bragg resonance versus grating thickness of an unslanted reflection grating recorded and replayed at oblique incidence with the Gaussian tapering harmonic index modulation of equation(43). The continuous green lines represents the PSM analytic formula (equation(42)) and the dashed lines represent a rigorous chain matrix computation. Three values of the index modulation are plotted: $n_1(0)$=0.02, $n_1(0)$=0.04 and $n_1(0)$=0.08. Gratings are recorded at 532nm and 20 degrees angle of incidence and played back at 490.3nm at 30 degrees. n_0=1.5,ω=3.

The diffraction efficiency at Bragg resonance is then given by

$$\eta_\sigma = \left|\frac{c_S}{c_R}\right| S(0)S^*(0) = \left|\frac{c_S}{c_R}\right| \tanh^2\left[\frac{\kappa\int_0^d \gamma(y)dy}{\sqrt{c_R|c_S|}}\right] \qquad (36)$$

Away from Bragg resonance we may write the diffraction efficiency for the case of the hyperbolically decaying fringe contrast of equation (25)

$$\eta_\sigma = \left|\frac{c_R}{c_S}\right| S(0)S^*(0) \qquad (37)$$

where

$$S(0) = \left(\frac{i\hat{\alpha}\vartheta}{a}\right)^{-\frac{1}{2}-\frac{\hat{\alpha}\kappa}{a}} \times$$

$$\frac{\left\{\begin{array}{l}(-1-ad)\Omega_0\hat{\alpha}\vartheta\left(\frac{i\hat{\alpha}\vartheta}{a}\right)^{\frac{1}{2}+\frac{\hat{\alpha}\kappa}{a}}\Omega_3\left(\vartheta\Omega_5+i\kappa\Omega_6\right)+ \\ \hat{\alpha}\vartheta\Omega_9\left(\begin{array}{l}\sqrt{\pi}\left(\frac{i\hat{\alpha}\vartheta}{a}\right)^{\frac{\hat{\alpha}\kappa}{a}}\Omega 1\left(\vartheta\Omega_5+i\kappa\Omega_6\right)+ \\ \left(-\sqrt{\pi}\left(\frac{i\hat{\alpha}\vartheta}{a}\right)^{\frac{\hat{\alpha}\kappa}{a}}\Omega_2+e^{\frac{i\hat{\alpha}\vartheta}{2a}}\sqrt{\frac{i\hat{\alpha}\vartheta}{a}}\Omega_4\right)\times \\ \left(i\kappa\Omega_7+(1+ad)\vartheta\Omega_8\right)\end{array}\right)\end{array}\right\}}{\sqrt{\frac{i\hat{\alpha}\vartheta}{a}}} \qquad (38)$$

$$\left\{\begin{array}{l}(-1-ad)\Omega_0\hat{\alpha}\vartheta\kappa\Omega_3\Omega_6 \\ +a\sqrt{\pi}\Omega_9\left(\begin{array}{l}-i\kappa\Omega_1\Omega_6+ \\ \Omega_2\left(i\kappa\Omega_7+(1+ad)\vartheta\Omega_8\right)\end{array}\right)\end{array}\right\}$$

with

$$\hat{\alpha} = \alpha\frac{\cos\theta_r}{\cos^2\theta_c} \qquad (39)$$

and where the omega functions are again given in Appendix A.

In the case of the π-polarization the PSM equations (3,6) can be written

$$\sin\theta_c \frac{\partial R}{\partial x} + \cos\theta_c \frac{\partial R}{\partial y} =$$
$$\frac{R}{2}\left\{2i\beta - \frac{\cos 2\theta_c}{n\cos\theta_c}\frac{\partial n}{\partial y}\right\} - \frac{S}{2}\left\{\frac{\cos 2\theta_c}{n\cos\theta_c}\frac{\partial n}{\partial y}\right\} \qquad (40)$$
$$\sin\theta_c \frac{\partial S}{\partial x} - \cos\theta_c \frac{\partial S}{\partial y} =$$
$$\frac{S}{2}\left\{2i\beta + \frac{\cos 2\theta_c}{n\cos\theta_c}\frac{\partial n}{\partial y}\right\} + \frac{R}{2}\left\{\frac{\cos 2\theta_c}{n\cos\theta_c}\frac{\partial n}{\partial y}\right\}$$

If we replace Kogelnik's constant by

$$\kappa \rightarrow \kappa \cos 2\theta_c \qquad (41)$$

then applying the same method as above we arrive at identical equations as derived for the σ-polarization. For example at Bragg resonance we may write

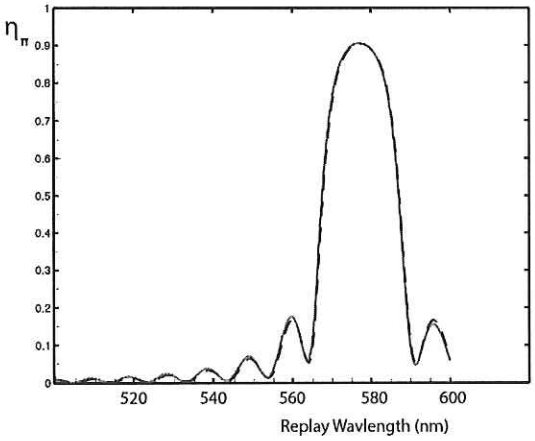

Fig.9. Diffraction efficiency versus replay wavelength for the hyperbolically decaying fringe contrast function of equation (43) and Fig.6. Recording wavelength 532nm. n_0=1.5. n_1=0.06, d=10 microns. Recording incidence angle is 20 degrees and replay incidence angle is 30 degrees. Blue dashed line is the analytic result of equation (42) and red line represents a rigorous chain matrix calculation.

$$\eta_\pi = \left|\frac{c_S}{c_R}\right| S(0)S^*(0) = \left|\frac{c_S}{c_R}\right| \tanh^2\left[\frac{\kappa\cos 2\theta_c \int_0^d \gamma(y)dy}{\sqrt{c_R|c_S|}}\right] \qquad (42)$$

To ascertain the accuracy of these formulae we use as a reference a rigorous numerical chain matrix calculation based on 10,000 discretized layers (6,10). Fig.8 shows the analogue of Fig.3 when reconstructed using a π-polarization reference beam having an incidence angle of 30 degrees. Here the grating equation is given by

$$n = n_0 + n_1 e^{-\frac{\omega y^2}{d^2}} \cos(2\alpha\beta y\cos\theta_r) \qquad (43)$$

Fig.9 likewise shows the analogue of Fig.7 when reconstructed by a π-polarization reference beam at an incidence angle of 30 degrees. Clearly both figures show excellent agreement between the rigorous numerical chain matrix calculation and the PSM model.

5.Discussion

Reflection HOEs and holograms recorded in a silver-halide emulsion can be subject to a fringe contrast that depends on the depth into the emulsion (1). Since wet processing is required, the development process starts from the top of the emulsion and the developer reaches the bottom rather later, resulting in higher silver density variation at the top of the emulsion as compared to that at the bottom. During the bleaching process to create a phase hologram, the density variations result in corresponding variations in δn, the index modulation, which gradually decreases throughout the depth of the emulsion.

The emulsion thickness for reflection holograms recorded in silver-halide emulsions is typically between 7 and 10 microns and in this case the δn variation may not be that significant. However in thicker gratings this is not the case. Indeed special processing techniques have been developed for *nuclear emulsions.*

A nuclear emulsion is an extremely thick photographic silver-halide emulsion in which elementary particle tracks are recorded directly as the particles pass through the emulsion (11-13). These very thick emulsions (up to 1 mm) require a uniform depth development through the entire emulsion in order to be useful. One solution to this problem has been to use special developers and to adjust the solution temperature in such a way that the developer penetrates the emulsion without having a developing effect on it. This can be achieved if the developer is kept at a low temperature during the penetration stage and if, at the offset of development, the temperature is increased. The technique has been applied to holography by Kaspar *et al.* (14). Holographic processing tests by one of the authors (HB), using a modified version of this technique, resulted in reflection holograms of a rather narrower spectral bandwidth.

In addition to silver-halide materials *photopolymer materials* are routinely used to record phase reflection gratings and holograms. The photopolymer material does not need wet processing - the image is actually formed automatically during the recording. A finished polymer hologram is almost free of absorption. However, the unexposed photopolymer material has rather high absorption caused by the sensitizing dyes. The absorption during recording can therefore affect index modulation, resulting in a variable fringe contrast.

In order to derive useful analytical expressions for the diffraction efficiency for reflection gratings having a depth-dependent fringe contrast we have used the PSM model (3-9). We have restricted the analysis here to the unslanted grating; but in fact the same techniques may be applied to gratings of finite slant.

Unfortunately there appear to be no actual measurements published in the literature concerning fringe contrast profiles. The closest studies are perhaps those of Ingwall et al (15,16) of Polaroid's DMP-128 photopolymer but although electron micrographs were presented in these papers of the cross-section of reflection gratings, no actual measurement of the fringe contrast profile was made. As such, we have applied the theoretical model developed in this paper to various fringe contrast profiles ranging from what one might typically expect under the most simplistic arguments to rather more extreme cases. Hopefully this approach will be seen to demonstrate the validity of our approach in the absence of exact experimental results. Indeed direct measurement of the fringe contrast profile is not at all simple. However an indirect measurement may perhaps be most easily inferred by using the theory developed here to match spectral measurements.

The PSM model is based on an application of the concept of Fresnel reflection as first suggested by Rouard in 1937 (17). The grating is decomposed into an infinite series of parallel stacked mirrors, each possessing an infinitesimal thickness; at each mirror the classical laws of Fresnel transmission and reflection are applied. In this way a reference wave, which illuminates the grating, provokes an infinite sum of secondary "Fresnel" waves, which add to form the diffractive response.

The PSM model can also be viewed as a type of differential generalization of the chain matrix method, which is often used in the numerical calculation of the optical properties of stratified media (10, 18, 19).

As we have seen, the PSM model lends itself rather easily to analyzing the case of a general fringe contrast profile as the underlying equations are valid for arbitrary index modulation. PSM would also seem the natural starting point for such an analysis as it seems to provide a somewhat better predictive model of most unslanted reflection gratings than that provided by conventional coupled wave theory (8). This is not to say that conventional coupled wave theory cannot be used to derive these results. It most certainly can, and in fact the equations derived from 2-wave coupled wave theory at Bragg resonance turn out to be identical to the PSM equations. Away from Bragg resonance the governing differential equations are only different in the definition of the coefficients. This is of course very reminiscent of the situation at constant fringe contrast.

The most important result of this paper is the derivation of a very general and simple analytic formula for the diffraction efficiency at Bragg resonance. Comparison of this result for even quite radical fringe contrast profiles shows extremely close agreement with rigorous numerical calculations. The theory tells us that at Bragg resonance we may always think of a reflection grating with variable fringe contrast as equivalent to a grating of constant fringe contrast having an effective thickness which is just a simple integral of the actual fringe contrast. Although we have restricted our attention to the unslanted grating, the analysis carries through identically to the case of finite slant as long as the normal finite-slant expressions for c_R, c_S and ϑ are now used (3).

Away from Bragg resonance we find that the PSM equations do not unfortunately lead to an analytic form that is valid for an arbitrary fringe contrast. The same situation occurs in a coupled wave analysis. However the special case of a hyperbolically decreasing fringe contrast is shown to lead to a rather complex, yet useful analytic solution. Once again, comparison of this result shows extremely close agreement with rigorous numerical solutions.

6.Conclusions

The PSM model has been used to analyze the process of diffraction occurring in volume reflection gratings in which fringe contrast is an arbitrary function of distance within the grating. Such variable fringe contrast profiles are expected to arise from diffusion processes occurring in the chemical processing of silver halide gratings and from optical absorption occurring in photopolymer gratings. General analytic expressions for diffraction efficiency at Bragg resonance have been obtained for the unslanted panchromatic lossless reflection grating at oblique incidence. These formulae have then been checked, for various diverse fringe contrast profiles with numerical solutions of the Helmholtz equation where exceptionally good agreement has been observed. Away from Bragg resonance the case of the hyperbolically decaying fringe contrast profile has been shown to lead to an analytic expression for the diffraction efficiency and this has again been compared successfully with numerical solutions of the Helmholtz equation.

Appendix A

The omega functions of equation (27) and equation (38) are given here in terms of confluent hypergeometric functions of the second kind, U, modified Bessel functions of the second kind, K, and generalized Laguerre polynomials, L. For equation (27)

$$\hat{\alpha} = \alpha \tag{44}$$

whereas for equation (38)

$$\hat{\alpha} = \alpha \frac{\cos\theta_r}{\cos^2\theta_c} \tag{45}$$

$$\Omega_1 = U\left[\frac{\hat{\alpha}\kappa}{a}, 1+\frac{2\hat{\alpha}\kappa}{a}, \frac{\mathrm{i}(1+ad)\hat{\alpha}\vartheta}{a}\right]$$

$$\Omega_2 = U\left[\frac{\hat{\alpha}\kappa}{a}, 1+\frac{2\hat{\alpha}\kappa}{a}, \frac{\mathrm{i}\hat{\alpha}\vartheta}{a}\right]$$

$$\Omega_3 = K_{\frac{1}{2}+\frac{\hat{\alpha}\kappa}{a}}\left[\frac{\mathrm{i}(1+ad)\hat{\alpha}\vartheta}{2a}\right]; \Omega_4 = K_{\frac{1}{2}+\frac{\hat{\alpha}\kappa}{a}}\left[\frac{\mathrm{i}\hat{\alpha}\vartheta}{2a}\right]$$

$$\Omega_5 = L^{1+\frac{2\hat{\alpha}\kappa}{a}}_{-\frac{a+\hat{\alpha}\kappa}{a}}\left[\frac{\mathrm{i}\alpha\vartheta}{a}\right]; \Omega_6 = L^{\frac{2\hat{\alpha}\kappa}{a}}_{-\frac{\hat{\alpha}\kappa}{a}}\left[\frac{\mathrm{i}\alpha\vartheta}{a}\right] \qquad (46)$$

$$\Omega_7 = L^{\frac{2\hat{\alpha}\kappa}{a}}_{-\frac{\hat{\alpha}\kappa}{a}}\left[\frac{\mathrm{i}(1+ad)\alpha\vartheta}{a}\right]$$

$$\Omega_8 = L^{1+\frac{2\hat{\alpha}\kappa}{a}}_{-\frac{a+\hat{\alpha}\kappa}{a}}\left[\frac{\mathrm{i}(1+ad)\alpha\vartheta}{a}\right]$$

$$\Omega_9 = \left(\frac{\mathrm{i}(1+ad)\hat{\alpha}\vartheta}{a}\right)^{\frac{1}{2}+\frac{\hat{\alpha}\kappa}{a}}; \Omega_0 = \mathrm{e}^{\frac{\mathrm{i}(1+ad)\hat{\alpha}\vartheta}{2a}}$$

References

1. H. I. Bjelkhagen, *Silver halide recording materials for holography and their processing*, Springer Series in Optical Sciences, Vol. **66** (Springer-Verlag 1993, 1995).
2. H. Kogelnik, "Coupled wave theory for thick hologram gratings," Bell Syst. Tech. J. **48**, 2909-2947 (1969).
3. D. Brotherton-Ratcliffe, "A treatment of the general volume holographic grating as an array of parallel stacked mirrors," J. Mod. Optics. **59**, 1113-1132 (2012).
4. D. Brotherton-Ratcliffe, "Analytical treatment of the polychromatic spatially multiplexed volume holographic grating," Appl. Opt. **51**, 7188-7199 (2012).
5. D. Brotherton-Ratcliffe, "A new type of coupled wave theory capable of analytically describing diffraction in polychromatic spatially multiplexed holographic gratings," Journal of Physics, Conference Series **415** (2013) 012034 doi:10.1088/1742-6596/415/1/012034.
6. H. Bjelkhagen and D. Brotherton-Ratcliffe, *Ultra-realistic imaging – advanced techniques in analogue and digital colour holography,* (CRC - Taylor and Francis 2012).
7. D. Brotherton-Ratcliffe, "Understanding diffraction in volume gratings and holograms," in *Holography - Basic Principles and Contemporary Applications*, E. Mihaylova, ed., Chap. 1 (INTECH, 2013).
8. D. Brotherton-Ratcliffe, L. Shi. A. Osanlou and P. Excell, "A comparative study of the accuracy of the PSM and Kogelnik models of diffraction in reflection and transmission holographic gratings," Opt. Express **22** (26) 32384-32405 (2014).
9. D. Brotherton-Ratcliffe, A. Osanlou and P. Excell, "Using the parallel-stacked mirror model to analytically describe diffraction in the planar volume reflection grating with finite absorption", Applied Optics Vol. **54**, pp. 3700–3707 (2015)
10. M. G. Moharam and T. K. Gaylord, "Chain-matrix analysis of arbitrary-thickness dielectric reflection gratings," J. Opt. Soc. Am. **72**, 187-190 (1982).
11. P. Demers, 'Cosmic ray phenomena at minimum ionization in a new nuclear emulsion having a fine grain, made in the laboratory' Cdn. J. Phys. **32**, 538-554 (1954).
12. J. F. Garfield, "Apparatus and a laboratory for processing thick nuclear track emulsions," Photogr. Sci. Eng. **2**, 85-90 (1958).
13. R. Diotallevi, E. Lamanna, A. Lucci, F. Meddi and G. Rosa, 'The laboratory for nuclear emulsion processing at Rome' Nota Interna No.775, Physics Institute, Univ. of Rome (1981)
14. F. G. Kaspar, R. L. Lamberts and C. D. Edgett, "Comparison of experimental and theoretical holographic image radiance," J. Opt. Soc. Am. **58**, 1289-1295 (1968).
15. R. T. Ingwall, M. Troll, and W. T. Vetterling, "Properties of reflection holograms recorded in Polaroid's DMP-128 photopolymer, " Proc. SPIE Vol. 747, 67-73 (1987).
16. R. T. Ingwall and M. Troll, "The mechanism of hologram formation in Polaroid's DMP-128 photopolymer, " Proc. SPIE Vol. 883, 94-101 (1988).
17. M. P. Rouard, "Etudes des propriétés optiques des lames métalliques très minces," Ann. Phys. (Paris) Ser. II **7**, 291-384 (1837).
18. F. Abeles, "Recherches sur la propagation des ondes électromagnétiques sinusoïdales dans les milieux stratifiés, Application aux couches minces," Ann. Phys. (Paris) **5**, 596-640 (1950).
19. O. S. Heavens, "Optical Properties of thin films," Reports on Progress in Physics, Vol **XXIII**, (1960), p1.